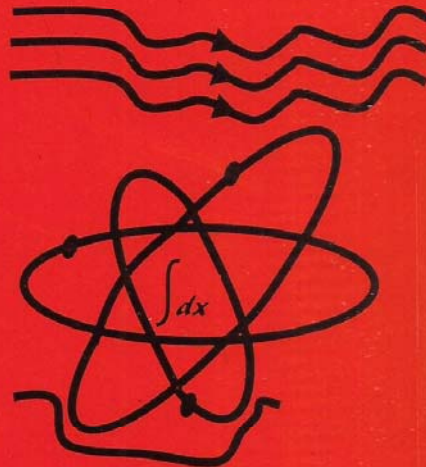


**V**olume **48**  
*Sept. & Nov., Issue, 2018*

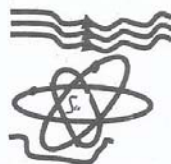
**J**OURNAL  
of the

NIGERIAN ASSOCIATION OF MATHEMATICAL PHYSICS



*Published by*

*Nigerian Association of Mathematical Physics*



**THE NIGERIAN ASSOCIATION OF MATHEMATICAL PHYSICS  
(NAMP)**

**Editorial Board for NAMP JOURNAL**

- Professor G. Babaji**,  
Department of Physics,  
Bayero University, Kano, Nigeria.
- Professor R. Akin-Ojo**,  
Department of Physics, University of Ibadan, Nigeria.
- Professor G. O. S. Ekhaguere**,  
Department of Mathematics,  
University of Ibadan, Nigeria.
- Professor A. O. E. Animalu**,  
Department of Physics,  
University of Nigeria, Nsukka, Nigeria.
- Professor G. C. Asomba**,  
Department of Physics,  
University of Nigeria, Nsukka, Nigeria.
- Professor E. O. Okeke**  
Department of Mathematics and Computer Science,  
Western Delta University,  
Oghara, Delta State, Nigeria.
- Professor J. O. A. Idiodi**,  
Department of Physics,  
University of Benin, Nigeria.
- Professor A. Nduka**  
Department of Physics,  
Federal University of Technology, Owerri, Nigeria.
- Professor Sunday Iyahen**  
Department of Mathematics,  
Benin Idahosa University, Benin City, Nigeria.

**Council of NAMP**

- Professor G. Babaji**/Bayero University Kano/Nigeria/Nigeria/President  
**Professor Vincent Asor**/Michael Okpara University of Agriculture, Umudike/Nigeria/Vice-President  
**Professor E.O. Oghre**/University of Benin, Benin City/Nigeria/Secretary  
**Dr. A.O. Popoola**/Osun State University, Osogbo/Nigeria/Treasurer  
**Professor John O.A. Idiodi**/University of Benin, Benin City/Nigeria/Editor-in-Chief

**Correspondence**

All correspondence relating to NAMP Publications and the submission of articles for publication  
Should be addressed to the **Editor-in-Chief**, whose address is:

**Professor John O.A. Idiodi**,  
Department of Physics,  
University of Benin, Benin City, Nigeria.  
Email: [jjiodi@hotmail.com](mailto:jjiodi@hotmail.com); Tel. +2348037994106

For further information, check our website: [www.nampjournals.org](http://www.nampjournals.org).

The Nigerian Association of Mathematical Physics, Sept. & Nov. Issue, 2018

journal of the nigerian association of mathematical physics

# JOURNAL

*of the*

NIGERIAN ASSOCIATION OF MATHEMATICAL PHYSICS

Vol. 48



## Contents: = = = = =

Null Controllability Of Fractional Integro-differential Systems In Banach Spaces with Distributed Delays In The Limited Control Powers	<i>P. A. Oraekie</i>	1
Computable Criteria For Null Controllability Of impulsive Quasi-Linear Fractional Mixed Volterra –Fredholm-Type Integro – Differential Systems In Banach Spaces With Multiple Delays In The Limited Control Powers.	<i>P. A. Oraekie</i>	11
On The Activities Of Unidirectional Nonlinear Water Waves On A Vertical Wall	<i>E.O. Okeke and V.E. Asor</i>	23
New Multiple Integral Collocation Methods For The Numerical Solution Of Fourth-Order Integro-Differential Equations	<i>A.O. Adewumi, O.M. Ogunlaran and A.F. Adebisi</i>	29
On Numerical Investigation And Assessment Of Variable Coefficient $C(x)$ Onairy Differential Equation	<i>Falade K.I, Tiamiyu A.T. and Muhammad M.Y.</i>	35
An Accurate Four-Point Hybrid Block Method for the Solution of General Third Order Differential Equations:	<i>Obarhua F. O. *, Kayode S. J. and Areo E. A.</i>	47
Numerical Solution Of Bagley-Torvik Fractional Differential Equation	<i>Olagunju A. S., Yakubu D. G., Komolafe E.Y, Abang M.O., and Raji M. T.</i>	57
On The Inverse Burr distribution: Its Properties and Applications	<i>J.E. Osemwenkhae and K.O. Iyenoma</i>	61
Investigating The Inverse Relationship Between Actuarial Liability And Discount Rates Under Gratuity Retirement Planning	<i>G.M. Ogungbenle and J.S. Adeyele</i>	67
Statistical Analysis Of Reported Cases Of Daily Road Accidents (Case Study Of University Of Iforin Teaching Hospital, Ilorin Kwara State)	<i>Ibrahim Wale Mohammed</i>	77
Buys-Ballof Modeling Of The External Reserves Of Nigeria	<i>George U. and Obasi E.J.</i>	85
Optimum Compromise Allocation In Multivariate Stratified Sampling Design With Gamma Cost Function: A Case Of Non-Response	<i>Abubakar Yahaya and Okon Ekom-Obong Jackson</i>	93
A Three State Markov Model of the Performance of a Banking Industry In Nigeria Stock Market: A Case Study Of Access Bank Plc	<i>M.T. Gana, U.Y. Abubakar, and Mohammed Abdullahi</i>	103

## Contents



255	Mathematical Model on the Transmission Dynamics of Meningococcal Meningitis With Vaccination <i>Momoh A.A., Kanuwa J. M., Washachi D.J. and Alhassan. A.</i>	111
261	Mathematical Modelling of the Dynamics of Hepatitis B Virus Infection in the Presence of Liver Size, Effector And Refractor Cells <i>A. A. Momoh, S. Z. Idris, U. Garba and Deborah Mathias</i>	123
267	Preventive Replacement Model of a Repairable Deteriorating System Subject To Three Types Of Failure <i>Salisu Murtala and Sale Ali</i>	137
275	Bifurcation Analysis of a Mathematical Model for Malaria Transmission Under treatment and Control <i>C.O. Udaya, E.O. Eze and G.C.E. Mbah</i>	141
285	Global Stability Analysis for the Mathematical Model of Dynamics of Diabetes Mellitus and Its Complications. <i>Aye P.O., Akinwande N.I., Kayode D.J. and Adebileje A.T.</i>	155
291	Risk Optimization in Diversification Strategy <i>Jayeola Dare</i>	161
297	Sensitivity Analysis for Production Planning Model and Its Application to Decision Making (A Case Study of Sunseed Nigeria Plc Zaria) <i>Kassim M.</i>	165
309	On The Performance of Floyd's Algorithm And All-Or-Nothing Assignment in Determining Shortest Paths For Commercial, Motoreycles Town Service <i>Nyor N., Idrisu M., Evans P. O. and P. N. Assi</i>	171
321	Existence Of Equilibrium Points Of Mathematical Model Of Transmission And Control Of Zika Virus Fever Dynamics <i>Adeyemo K.A., Akinwande N.I., Kuta F.A. and Abdulrahman S.</i>	181
331	Mathematical Models Of Road Accident In A Developing Economy <i>Hamza Mansur, U.L. Okafor and Bashir Yusuf</i>	189
337	Selecting The Best Initial Method for a Transportation Problem <i>Onah I. S. and Osedume N.I.</i>	199
343	A General Potential for Molecular Dynamics of Ion-Sputtered Surfaces <i>Akande Raphael O. and Oyewande Emmanuel O.</i>	209
347	Theoretical Monitoring of Energy Transport on Solid Surfaces at Nano-Metric Scales <i>Akande Raphael O.</i>	219
353	Topographic Phase Boundary Shifts and Saturation for Anisotropic Ion Straggle During Sputter Etching <i>Emmanuel O. Yewande and Raphael O. Akande</i>	227
357	Preliminary Interpretation of Magnetic Survey Undertaken in Michael Okpara University of Agriculture (MOU)AU, Umudike, Abia State. <i>Igboekwe M. U., Ohakwere-Eze M. C., Anyadiegwu F. C., Ahamefule C. Y. and Eme U. K.</i>	233
363	Determination Of Radionuclide Concentration Levels In Some Bathing Soaps Used In Nigeria <i>A. H. Ojelabi and N.N. Jibiri</i>	239
367	Generalized Dynamical Gravitational Scalar Potential For Static Homogeneous Spherical Distribution Of Mass Using Taylor Series Approach <i>Okpara P. A., Umahi E. A. and Oboma, D.N.</i>	243
373	Similarity in solutions of Nonlinear Stretched Biomagnetic Flow and Heat Transfer with Signum Function and Temperature Power Law Geometry <i>Ogundola S. and Omeke N.E.</i>	247

## Contents

Radial Distance and Azimuthal Angle Varying Tensor Field Equation Exterior to Homogeneous Spherical Mass Distribution <i>M.U. Sarki, W.I. Lumbi and I.I. Ewa</i>	255
Location of Triangular Equilibrium Points for The Binary Lalande 21258 System In The Restricted Problem Of Three Bodies <i>J. M. Gyegwe, S.O. Imoni, V. E. Aguda, H.O. Edoghanya</i>	261
Investigation of Rock Physics In Fracture Pressure Prediction: Examples From The Niger Delta Central Swamp And Shallow Offshore Depobelts <i>Ogagarue D.O. and Ogbe O.B.</i>	267
An Assessment of The Impact of Climate Change on Properties Within Victoria Island, Eti-Osa Local Government Area, Lagos. <i>Iruobe, P. O., Ugwuejim S. C. and Nworah, J. C.</i>	275
Geophysical Investigation of Mineral Occurrences In Usen, Ovia South West I.G.A, Nigeria. <i>Enoma N., Emmanuel B.H., Edo T.M. and Ikuybogie F.O.</i>	285
Assessment of Fade Depth and Geoclimatic Factor for Microwave Frequency Application In Ondo City, Nigeria. <i>Ojo O.L. and Adenodi R.A.</i>	291
Resistivity Survey For Groundwater In Parts Of Enugu South Local Government Area, Enugu State <i>Nneji E. G., Anyadiegwu F. C., and Ijeh B. I.</i>	297
Evaluation Of The Modelling Of Chlorine Residual Concentration In An Automated Treatment Plant Of A Water Distribution System <i>Audu, H.A.P. and Ikhafia, O. P.</i>	309
Analysis Of Electric Power Losses In Distribution Lines: A Case Study Of Jos And Environ. <i>D.N. Dawuk, S.D. Yaulu, B.D. Daben, B. Barnabas, and M.Y. Mafuyai</i>	321
Numerical Determination Of The Effects Of Pouring Temperature And Mold Preheat Temperature On The Solidification Time In Centrifugal Casting <i>Erhunmwun J. D., Akpobi J. A. and Osunde T. A.</i>	331
Application of Response Surface Methodology to Predict The Heat Input of Tig Mild Steel Welds <i>Uwoghren F.O. and Ehiorobo J.O.</i>	337
Application of Artificial Neural Network To Predict The Heat Input Of Tig Mild Steel Welds <i>Uwoghren F.O. and Achebo J.I.</i>	343
On Improving Power Supply Flexibility <i>Ekpa T. K., Sani S., Hasssan A. S. and Kalyankolo Z.</i>	347
Designing Picogrids for Non-Smartphones: Sufficient Conditions <i>Sani S., Ekpa T. K., Hassan A. S. and Kalyankolo Z.</i>	353
Determination Of The Viscosity Of Local Honey By Falling-Sphere Viscometer <i>A. Olatunji, M. Adebisi and C.J. Olowookere</i>	357
Synthesis and electrochemistry of $3D Na_xSNO_{1-x}g$ ( $0.3 \leq x \leq 0.4$ ) Composite Electrode for Supercapacitor Application. <i>M. Alpha., U.E. Uno., Isah K.U., Ahmadu U.</i>	363
Development Of A Low-Cost Microcontroller Based Lux-Meter With Photoresistor Sensor <i>Obagade T.A., Alamuoye I.H. and Fatile J.A.</i>	371

**SYNTHESIS AND ELECTROCHEMISTRY OF 3D  $\text{Na}_x\text{SnO}_{1-x}/\text{G}$  ( $0.3 \leq x \leq 0.4$ )  
COMPOSITE ELECTRODE FOR SUPERCAPACITOR APPLICATION.**

*M. Alpha., U.E. Uno., Isah K.U. and Ahmadu U.*

Department of Physics, Federal University of Technology Minna, P.M.B 65, Minna, Nigeria

**Abstract**

*Studying the electrochemistry of  $\text{Na}_x\text{SnO}_{1-x}/\text{G}$  composite ( $0.3 \leq x \leq 0.4$ ) as an electrode material for supercapacitor application, the reduce graphene oxide (G) was synthesized using an improved modified Hummer's method and the composites electrode material using hydrothermal reduction method. The electrode  $\text{Na}_x\text{SnO}_{1-x}$  ( $x = 0.4$ ) gives the highest specific capacitance of 103.5 F/g, energy density of 26.4Wh/kg and power density of 205.9 W/kg after one cycle and after 1000 cycles CV test, it gives the highest capacitance efficiency, equivalent to 94.7 % capacitance retention. The electrode  $\text{Na}_x\text{SnO}_{1-x}$  ( $x = 0.3$ ) gives the lowest specific capacitance of 102.6 F/g, energy density of 25.5Wh/kg and power density of 152.1 W/kg after one cycle and after 1000 cycles CV test, it gives the lowest capacitance efficiency, equivalent to 93.9 % capacitance retention. This research highlighted the importance of introducing Na doped SnO in the network of the reduce graphene oxide in order to enhance the electrochemistry of the composite electrode for supercapacitor application.*

**Keywords:** Reduce Graphene Oxide, Capacitance, Energy density, Power density, Electrode

**I. Introduction**

The increasing demand for a reliable and sustainable source of energy for technological growth and development has facilitated increase in funding energy related research. The increase in the world population and advancement in technology has also created an increase in the global demand for energy use ranging from small scale domestic applications (in terms of personal use) to large scale industrial applications for transport and manufacturing purposes.

This has led to an increasing interest in renewable energy-based research for generating a much cleaner and safer energy generation/conversion system. Therefore, there is also a need to build a reliable and efficient energy storage system to preserve the excess generated power for use when required for specific applications. Such storage system must possess high energy and high power densities in order to provide a robust storage capacity alone with an instantaneous/rapid delivery capability respectively. Nowadays, semiconductor metal oxides, carbon materials, and conducting polymers are applied as basic pillars for electrodes [1], [2]. The carbonaceous substances indicate best physical and chemical properties while the polymers with conductivity properties present high pseudo capacitance, low cost, conductivity, best energy density. However, EDLCs have the best pore-size and surface area. Then, pseudocapacitors with transition metal oxides materials can present excellent specific capacitance and energy storage density. Carbon materials have been applied as framework to support Na-ion host materials, such as phosphorous [3], Sn-based compounds [4], in order to increase the electronic conductivity of electrode materials during charge/discharge processes. Graphene has been widely used as effective building blocks for these purposes, owing to its high electronic conductivity, two-dimensional structure with high surface area, and flexibility. In order to meet the demand of high energy storage, numerous efforts have been devoted to enhancing the electrochemical performance of the graphene-based composite materials based on rational material manipulations [5].

It is very important to note that among tin oxide compounds, tin dioxide ( $\text{SnO}_2$ ) and tin monoxide ( $\text{SnO}$ ) have attracted much attention due to their potential applications in optoelectronic devices such as solar cells, displays, sensors, and complementary oxide-thin film transistors [6]. The existence of different oxidation states in tin ion makes it more beneficial to have non stoichiometric tin oxide phases.  $\text{SnO}_2$  is generally an n-type semiconductor due

Corresponding Author: Alpha M., Email:

Tel: +2348062459364

to the existence of intrinsic defects such as oxygen deficiencies and tin interstitials, but SnO exhibits p-type conductivity with a relatively high hole mobility originated from the tin vacancy. From the literature concerned, most research work in the past electrochemistry has paid attention to SnO<sub>2</sub>, whereas experimental reports on SnO are fewer because of its meta-stability and tendency to transform into SnO<sub>2</sub> at high oxygen pressures [7]. However, interest in SnO has been recently resurged because of the difficulty in obtaining high quality p-type oxide semiconductor such as p-type-doped NiO and CuO. It is believed that the p-type conductivity of SnO can be further improved by proper doping [8], [9].

Pure graphene can be modified by oxygen or other heteroatoms to show increased electrochemical capacitance. Such a modification is attributed to the redox activity enabled by the hetero atoms, known as pseudocapacitance which is the same as or comparable to the CH11604E Electrochemical with the common capacitive behaviour that is featured by rectangular cyclic voltammograms [10]. It is commonly considered that the Faradaic to result from electrode surface confined electron transfer reactions and hence is Faradaic in nature [11]. However, the electrode configuration of rectangular CVs of pseudocapacitance are in contrast to those peak-shaped CVs that can be predicted from the Nernst equation for single or multiple electron transfer reactions in surface confined battery-type materials. The differences between the two electrode configurations for Faradaic capacitive and Faradaic Nernstian electrode reactions are claimed to result from, respectively, the transfer of partially delocalised and localised valence electrons, although no theoretically justified explanation has yet been reported [12]. However, current studies on laboratory made graphene oxides (GOs) have not yet revealed well-defined atomic structures which bring difficulties to resolve the electronic structures. Further, oxygen in GOs is known to only exist in a few forms [13].

## 2. Experiment

### 2.1 Methods

The Reduced Graphene Oxide was synthesized using modified Hummer's methods and the composite material using hydrothermal reduction method at Advanced Chemistry Laboratory, Sheda Science and Technology Complex (SHESTOC), Abuja, Nigeria. All apparatus for the synthesis were washed with distilled water and then dried in an electric oven at 60 °C for 30 mins before used.

#### 2.1.1 Synthesis of Reduced Graphene Oxide (G)

5g of graphite, 2.5g of NaNO<sub>3</sub> and 115 mL H<sub>2</sub>SO<sub>4</sub> (98%) were added together and stirred for 30 min using a magnetic stirrer. The mixture was then transferred into an ice bath, then 15 g KMnO<sub>4</sub> was added slowly to mixture and maintained at below 20 °C, after the KMnO<sub>4</sub> was added, the temperature was then raised to 35 °C and stirred again for another 30 min. 230 mL of distilled water and ascorbic acid (5 mg dispersed in 10 mL of water to produce a 0.5 mg mL<sup>-1</sup>) to aid reduction was then added slowly to the mixture and temperature raised to 98 °C and stirred for another 15 min. At the end of the 15 min, 400 mL distilled water and 50 mL H<sub>2</sub>O<sub>2</sub> at 30% was added to the mixture then filtered and then washed with 1 M HCl then with 100 mL DI water and we get a cake of the reduced graphene oxide and dried in an electric oven for 60 min.

#### 2.1.2 Synthesis of Na doped SnO reduced graphene oxide (Na<sub>x</sub>SnO<sub>1-x</sub>/G) composite (0.3 ≤ x ≤ 0.4)

10 mg of the G was dispersed in 20 mL of water to produce a 0.5 mg mL<sup>-1</sup> completely water dispersed G.

i. G solution (0.5 mg mL<sup>-1</sup>) was mixed with 10 mL of water containing (7 mg SnCl<sub>2</sub>·2H<sub>2</sub>O and 3 mg NaNO<sub>3</sub>); ascorbic acid (5 mg dispersed in 10 mL of water to produce a 0.5 mg mL<sup>-1</sup>) to aid reduction and 10 mL of ethanol to aid homogeneity for the synthesis of Na<sub>0.3</sub>SnO<sub>0.7</sub>/G composite

ii. G solution (0.5 mg mL<sup>-1</sup>) was mixed with 10 mL of water containing (6 mg SnCl<sub>2</sub>·2H<sub>2</sub>O and 4 mg NaNO<sub>3</sub>); ascorbic acid (5 mg dispersed in 10 mL of water to produce a 0.5 mg mL<sup>-1</sup>) to aid reduction and 10 mL of ethanol to aid homogeneity for the synthesis of Na<sub>0.4</sub>SnO<sub>0.6</sub>/G composite.

The whole mixtures in (i, ii.) were sonicated at 60 °C for 3 h in a bath sonicator. After sonication the sample is then dried in an electric oven at 60 °C for 60 min.

## Results

### 1. Results

The structural properties were investigated using SEM.

#### 1.1 Raman

Figure 1 gives the

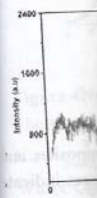


Figure 1 Raman

The Raman characteristic bands of reduced graphene oxide and its parent graphite. The G band is at 1580 cm<sup>-1</sup> and the D band is at 1350 cm<sup>-1</sup> [5].

From figure 1, the Raman intensity ratio of the G band to the D band has been calculated and it has been found that the ratio is 1.0, which indicates that the reduced graphene oxide is of high quality.

ductivity and  
 k in the past  
 tendency to  
 cause of the  
 ed that the p-

such a gain or  
 r comparable  
 y considerable  
 however, the  
 Nernst Law  
 between the  
 : transfer of  
 een reported  
 fined atomar  
 exist in a few

aterial using  
 SHESTCO  
 em at 60 °C

odic state  
 at below 20  
 230 ml of  
 an was then  
 ant. 400 ml  
 with 100 ml.

the acid  
 with 50 ml  
 the acid  
 with 50 ml  
 the acid  
 with 50 ml

363-370

### 2.1.3 Electrochemical Analysis

The electrochemical analyses of the samples were carried using Cyclic Voltammetry and Electrochemical Impedance Spectroscopy (EIS) tests from a CHI604E Electrochemical Analyser, controlled by EC-Lab VIO.37 software. The CHI604E Electrochemical Analyser is an electronic instrument designed to control the potential difference (E) applied to the working electrode (WE) with a current flow (in form of either a half cell or a full cell), a reference electrode (RE) with no current and the counter electrode (CE) through which current leaves the electrolyte while measuring the potential difference between the WE and RE.

The CHI604E Electrochemical Analyser generates characteristic cyclic voltammetry curves which give us information on the possible thermodynamics of electrochemical reactions of the system. All tests in this study were carried out in a three electrode configuration with the active material serving as the working electrode, a carbon rod serving as the counter electrode and Ag/AgCl serving as the reference. A 2 M KOH aqueous solution serve as the electrolyte which provides a medium for current flow and ion interaction. Although the nature of electrolyte is very important for an efficient enhancement of the performance of supercapacitors, comparison of different electrolyte types is not within the scope of this work.

## 3. Results and Discussion

### 3.1 Results and Discussion on Structural properties

The structural properties of the composite materials were analysed using the following characterisation; the Raman analysis and SEM.

#### 3.1.1 Raman analysis

Figure 1 gives the Raman spectra of the  $\text{Na}_x\text{SnO}_{1-x}$  ( $0.3 \leq x \leq 0.4$ ) graphene composites.

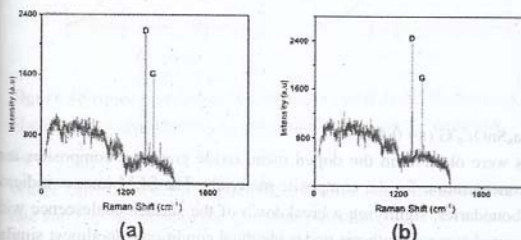


Figure 1 Raman spectra for (a)  $\text{Na}_x\text{SnO}_{1-x}/\text{G}$  ( $x=0.3$ ), (b)  $\text{Na}_x\text{SnO}_{1-x}/\text{G}$  ( $x=0.4$ )

The Raman spectra for the samples were obtained using OriginPro 2018 software and provide the best signature for characterisation of graphene samples and composites. The D band is the defects and disorder mode in the reduced graphene oxide and its composite material, while the G band is the  $\text{sp}^2$ -bonded vibration from carbon atoms (hexagonal lattice of graphite). The G and the D band are due to the bond stretching of all pairs of  $\text{sp}^2$  atoms and the vibrating modes of the  $\text{sp}^2$  bond [5].

From figure 1, the Raman shift for the composites give a D band value of about  $1348 \text{ cm}^{-1}$  and a G band value of about  $1500 \text{ cm}^{-1}$ . The Raman shift gives the  $I_D/I_G$  intensity ratio of 1.04. From figure 1 a shift of the D band intensity was observed for all the composites. This shift may have originated from structural distortion of the reduce graphene oxide [12] this may have been caused by the different bond distances of C-C atom and C-Na, C-Sn atoms owing to the introduction of the 3D doped



metal oxide in graphene networks. The Na dopants interact with the Sn<sup>2+</sup> providing additional active sites in the composite material which results in a strong coupling between the metal species and the reduce graphene oxide, resulting in shift in the D band. The shift in the D band intensity may also be due to slight change in temperature during the synthesis of the composite material.

From the relative high intensities of the D and G band, it can be concluded that the size of the sp<sup>2</sup> domains increase during the reduction of the graphene oxide. From figure 1, decrease in the intensities of the G band relative to the D band was observed for the composite material, this demonstrated that defect are more easily introduced into thinner reduced graphene oxide sheet which is as a result of the stretching of the sp<sup>2</sup> atom, which can be attributed to the presents of the 3D doped metal oxide within the layers of the graphene, this agrees with the report by [14]. This decrease in the G band intensities relative to D band in the composites materials reveals the disorder present in the sample, which can facilitate the trapping of ions from the electrolyte. The present of only D and G band in the composite material is a clear indication of the incorporation of the doped metal oxide into the reduce graphene oxide and this reflect the good crystallinity of the doped metal oxide in the composite material.

3.1.2 SEM Analysis

Figure 2 give the SEM images of Na<sub>x</sub>SnO<sub>1-x</sub>/G (x=0.3), Na<sub>x</sub>SnO<sub>1-x</sub>/G (x= 0.4),

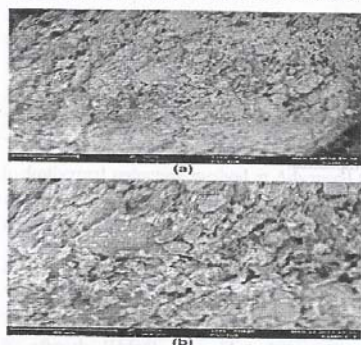


Figure 2 SEM images for (a) Na<sub>x</sub>SnO<sub>1-x</sub>/G (x=0.3) (b) Na<sub>x</sub>SnO<sub>1-x</sub>/G (x= 0.4)

Figure 2, a relatively uniform porous surface structures were observed in the doped metal oxide graphene composites and were observed to increase with increase in the doping concentration for the composite materials. The SEM images indicate that there was a slight increase in the number of grain boundaries, signifying a breakdown of the surface coalescence with increasing dopant concentration. However, since all the samples were synthesis under identical conditions, an almost similar microstructure and surface morphology was seen in all the doped metal reduce graphene electrode composites irrespective of the doping concentration.

Graphene layers interacting by means of van der Waals forces [15] and form an open pore system, through which electrolyte ions can easily access the surfaces of the graphene, which facilitate the formation of electric double layers and improve the electrochemical utilization of Na, and Sn nanoparticles into the network of the composite electrode. The doped metal oxides improve the accessibility due to their metal-cation and regular 3D dispersion in the structure of the electrode. Agglomeration adversely affects the performance of the reduced graphene oxide as an electrode by preventing electrolyte ions from penetrating into the reduced graphene oxide layers [16]. The doped metal oxide is being used as a spacer to prevent agglomeration, and thus avoid the loss of their high active surface area which ensures high electrochemical utilisation of the reduced graphene oxide and also contribute to the total capacitance. The SEM images in figures 2 shows that the doped metal oxide is sandwiched chemically within the layers of the reduced graphene oxide, resulting into 3D architecture material and reveals good quality dispersion. The lateral grain size of the reduced graphene oxide and composites material exhibits a wide distribution, ranging from 80 μm to 100 μm.

2 Results and the electrochem electrochemical the cyclic volta rate of 100 mVs spectroscopy an

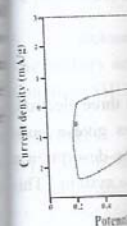


Figure 3 Cyclic

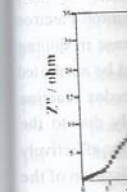


Figure 4 Nyq

The specific  $C_{sp} = \frac{S}{2mk(E)}$  Where  $C_{sp}$  is rate and E is The energy  $E_D = \frac{1}{8} C_{sp}$  Where C is The power i dielectric m associated  $P_D = \frac{1}{4X(ES}$  Where ESF resistance ( from the el

3.2 Results and Discussion on Electrochemical Analysis

The electrochemical properties of the composite materials were analysed using Cyclic Voltammetry (CV) and the Electrochemical Impedance Spectroscopy (EIS) analysis.

The cyclic voltammograms from the Cyclic Voltammetry analysis for  $\text{Na}_x\text{SnO}_{1-x}/\text{G}$  ( $x=0.3$ ) and  $\text{Na}_x\text{SnO}_{1-x}/\text{G}$  ( $x=0.4$ ) at a scan rate of  $100 \text{ mVs}^{-1}$ , current density of  $100 \text{ mA/g}$  is given in figure 3. The Nyquist plot from the Electrochemical Impedance Spectroscopy analysis for  $\text{Na}_x\text{SnO}_{1-x}/\text{G}$  ( $x=0.3$ ) and  $\text{Na}_x\text{SnO}_{1-x}/\text{G}$  ( $x=0.4$ ) composites electrode materials is given in figure 4

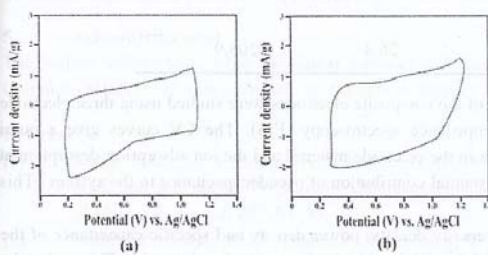


Figure 3 Cyclic Voltammogram for (a)  $\text{Na}_x\text{SnO}_{1-x}/\text{G}$  ( $x=0.3$ ) (b)  $\text{Na}_x\text{SnO}_{1-x}/\text{G}$  ( $x=0.4$ )

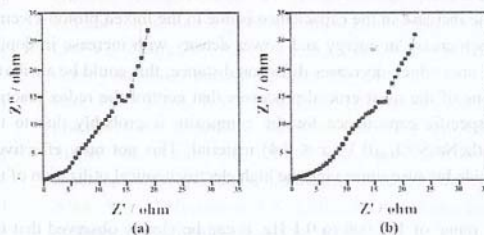


Figure 4 Nyquist plot for (a)  $\text{Na}_x\text{SnO}_{1-x}/\text{G}$  ( $x=0.3$ ) (b)  $\text{Na}_x\text{SnO}_{1-x}/\text{G}$  ( $x=0.4$ )

The specific capacitance ( $C_{sp}$ ) was calculated using the equation;

$$C_{sp} = \frac{S}{2mk(E)} \tag{1}$$

Where  $C_{sp}$  is the specific capacitance, S is the total charge surface area, m is the mass of the electrode material, k is the scan rate and E is the value of the electrode potential.

The energy density ( $E_D$ ) and power density ( $P_D$ ) were calculated using equations

$$E_D = \frac{1}{8} C_{sp} V^2 \tag{2}$$

Where C is the specific capacitance in F/g, V is the electrode potential in volts

The power is the energy expended per unit time and since the capacitor usually consists of the current collector, electrode and dielectric material, there will be an associated equivalent series resistance (ESR) from these extra components. As such; the associated maximum power density the cell can deliver is expressed as:

$$P_D = \frac{1}{4X(ESR) M} V^2 \tag{3}$$

Where ESR is the equivalent series resistance and M is the total mass of active material. The values of the equivalent series resistance (ESR) for the composites electrodes were obtained from the Nyquist plot in figure 4. The summary of the results from the electrochemical analysis is given in table 1.

Table 1 Summary of results from electrochemical analysis for one cycle

Composite	Mass (g)	$C_p$ (F/g)	ERS ( $\Omega$ )	$E_D$ (Wh/kg)	$P_D$ (W/kg)
$\text{Na}_x\text{SnO}_{1-x}/\text{G}$ ( $x=0.3$ )	0.151	102.6	4.0	25.5	152.1
$\text{Na}_x\text{SnO}_{1-x}/\text{G}$ ( $x=0.4$ )	0.161	103.5	3.0	26.4	205.9

The electrochemical properties and capacitance measurement of the composite electrodes were studied using three electrode system by cyclic voltammetry (CV) and electrochemical impedance spectroscopy (EIS). The CV curves give a quasi-rectangular shape due to the kinetics of electron transportation in the electrode material and the ion adsorption-desorption at the electrode and electrolyte interface and also due to the substantial contribution of pseudocapacitance to the system. This also agrees with report from [17].

From table 1, it was observed that there was increase in the energy density, power density and specific capacitance of the composites electrodes with increase in doping concentration of the cations (Na) in the composite electrodes. This is due to the expansion of the active sites when the 3D  $\text{Na}_x\text{SnO}_{1-x}$ , ( $0.3 \leq x \leq 0.4$ ) materials were introduced into the network of the reduce graphene oxide. This agrees with the work of [8]. The increase in the capacitance is due to the mixed proton-electron conductivity from the cations and the electrolyte ions. This increase in energy and power density with increase in doping concentration is also attributed to increase in charge surface area which decreases diffusion distance; this could be attributed to high  $\text{Na}^+$  diffusion coefficient, since ions diffusion is one of the most crucial processes that control the redox reaction within the electrode material [3]. The greatly enhanced specific capacitance for the composite is probably due to the synergetic effect between the reduce graphene oxide and the  $\text{Na}_x\text{SnO}_{1-x}$  ( $0.3 \leq x \leq 0.4$ ) material. This not only effectively inhibit the stacking/agglomeration of the reduce graphene oxide but also improving the high electrochemical utilization of the composites electrodes.

EIS measurement was carried within the probed frequency range of 100,000 to 0.1 Hz. It can be clearly observed that the impedance curves from the figure 4 consist of an arc and followed by a slanted line in the low frequency region. While in the high frequency region, the intercept of the semi circle on the real axis of the Nyquist plot represent the solution equivalent series resistance which can be correlated to the Ohmic resistance of the electrolyte in the system and the charge transfer resistance between interface of the electrode materials and the electrolyte. The Warburg impedance is related to the diffusional impedance of the electrochemical system which is employed to fit the straight line at the intermediate frequency, followed by a near vertical line at the lower frequency region [18-23]. From table 1, a decrease in ESR for all composite with increase in doping concentration was observed. This is due to the increase in the current response with increase in doping concentration. The decrease in the value of the ESR implies, the improve conductivity of the composite electrode and this enhances their capacitive performance, which is in accordance to the results obtained from the CV measurement. This decrease in ESR resulted in the increase in power density for the composite electrodes.

The cyclic stability of the electrode material is a crucial and important parameter to rank the performance of the energy storage application [19, 24]. The electrochemical stability of the composites electrodes were evaluated by repeating the CV test between 0.0 and 1.3 V at a scan rate of 100 mV/s for 1000 cycles under the same condition of the electrochemical set-up applied for one cycle. The composites electrode showed a greatly improved cycling stability and demonstrated the positive synergetic effect of  $\text{Na}_x\text{SnO}_{1-x}$  ( $0.3 \leq x \leq 0.4$ ) material with the reduce graphene oxide as composite electrode to meet the requirement for high energy and power density. The electrodes showed greatly improved cycling stability and demonstrated the positive synergetic effect of  $\text{Na}_x\text{SnO}_{1-x}$  ( $0.3 \leq x \leq 0.4$ ) material with the reduce graphene oxide as composite electrode to meet the requirement for high energy and power density. The electrode  $\text{Na}_x\text{SnO}_{1-x}/\text{G}$  ( $x=0.4$ ) after 1000 cycles CV test, it gives 98.0 F/g with the highest capacitance efficiency, equivalent to 94.7 % capacitance retention. The electrode  $\text{Na}_x\text{SnO}_{1-x}/\text{G}$  ( $x=0.3$ ) after 1000 cycles CV test, it gives 96.3 F/g with the lowest capacitance efficiency, equivalent to 93.9 % capacitance retention.

## Conclusion

The electrode  $\text{Na}_x\text{SnO}_{1-x}/\text{G}$  ( $x=0.4$ ) after 1000 cycles CV test, it gives 98.0 F/g with the highest capacitance efficiency, equivalent to 94.7 % capacitance retention. The electrode  $\text{Na}_x\text{SnO}_{1-x}/\text{G}$  ( $x=0.3$ ) after 1000 cycles CV test, it gives 96.3 F/g with the lowest capacitance efficiency, equivalent to 93.9 % capacitance retention.

## Acknow

The authors acknowledge the support of the Nigerian Association of Mathematical Physics (NAMAP) for the complex (SHES).

## References

- [1] Vinod, et al. Synthesis and electrochemical properties of  $\text{Na}_x\text{SnO}_{1-x}/\text{G}$  ( $x=0.3$ ) composite electrode. *Journal of Materials Science: Materials Chemistry and Physics*, 2018, 19(1), 1-10.
- [2] Bidhan, et al. Synthesis and electrochemical properties of  $\text{Na}_x\text{SnO}_{1-x}/\text{G}$  ( $x=0.4$ ) composite electrode. *Journal of Materials Science: Materials Chemistry and Physics*, 2018, 19(1), 1-10.
- [3] Qian, et al. Synthesis and electrochemical properties of  $\text{Na}_x\text{SnO}_{1-x}/\text{G}$  ( $x=0.3$ ) composite electrode. *Journal of Materials Science: Materials Chemistry and Physics*, 2018, 19(1), 1-10.
- [4] Liu, et al. Synthesis and electrochemical properties of  $\text{Na}_x\text{SnO}_{1-x}/\text{G}$  ( $x=0.4$ ) composite electrode. *Journal of Materials Science: Materials Chemistry and Physics*, 2018, 19(1), 1-10.
- [5] Hsu, et al. Synthesis and electrochemical properties of  $\text{Na}_x\text{SnO}_{1-x}/\text{G}$  ( $x=0.3$ ) composite electrode. *Journal of Materials Science: Materials Chemistry and Physics*, 2018, 19(1), 1-10.
- [6] Mel, et al. Synthesis and electrochemical properties of  $\text{Na}_x\text{SnO}_{1-x}/\text{G}$  ( $x=0.4$ ) composite electrode. *Journal of Materials Science: Materials Chemistry and Physics*, 2018, 19(1), 1-10.
- [7] Ali, et al. Synthesis and electrochemical properties of  $\text{Na}_x\text{SnO}_{1-x}/\text{G}$  ( $x=0.3$ ) composite electrode. *Journal of Materials Science: Materials Chemistry and Physics*, 2018, 19(1), 1-10.
- [8] M, et al. Synthesis and electrochemical properties of  $\text{Na}_x\text{SnO}_{1-x}/\text{G}$  ( $x=0.4$ ) composite electrode. *Journal of Materials Science: Materials Chemistry and Physics*, 2018, 19(1), 1-10.
- [9] A, et al. Synthesis and electrochemical properties of  $\text{Na}_x\text{SnO}_{1-x}/\text{G}$  ( $x=0.3$ ) composite electrode. *Journal of Materials Science: Materials Chemistry and Physics*, 2018, 19(1), 1-10.
- [10] E, et al. Synthesis and electrochemical properties of  $\text{Na}_x\text{SnO}_{1-x}/\text{G}$  ( $x=0.4$ ) composite electrode. *Journal of Materials Science: Materials Chemistry and Physics*, 2018, 19(1), 1-10.
- [11] I, et al. Synthesis and electrochemical properties of  $\text{Na}_x\text{SnO}_{1-x}/\text{G}$  ( $x=0.3$ ) composite electrode. *Journal of Materials Science: Materials Chemistry and Physics*, 2018, 19(1), 1-10.
- [12] J, et al. Synthesis and electrochemical properties of  $\text{Na}_x\text{SnO}_{1-x}/\text{G}$  ( $x=0.4$ ) composite electrode. *Journal of Materials Science: Materials Chemistry and Physics*, 2018, 19(1), 1-10.
- [13] K, et al. Synthesis and electrochemical properties of  $\text{Na}_x\text{SnO}_{1-x}/\text{G}$  ( $x=0.3$ ) composite electrode. *Journal of Materials Science: Materials Chemistry and Physics*, 2018, 19(1), 1-10.
- [14] L, et al. Synthesis and electrochemical properties of  $\text{Na}_x\text{SnO}_{1-x}/\text{G}$  ( $x=0.4$ ) composite electrode. *Journal of Materials Science: Materials Chemistry and Physics*, 2018, 19(1), 1-10.

#### 4. Conclusion

The electrode  $\text{Na}_x\text{SnO}_{1-x}$  ( $x = 0.4$ ) gives the highest specific capacitance of 103.5 F/g, energy density of 26.4Wh/kg and power density of 205.9 W/kg after one cycle and after 1000 cycles CV test, it gives the least capacitance efficiency, equivalent to 94.7 % capacitance retention.

The electrode  $\text{Na}_x\text{SnO}_{1-x}$  ( $x = 0.3$ ) gives the lowest specific capacitance of 102.6 F/g, energy density of 25.5Wh/kg and power density of 152.1 W/kg after one cycle and after 1000 cycles CV test, the electrode material  $\text{Na}_x\text{SnO}_{1-x}$  ( $x = 0.3$ ) gives the highest capacitance efficiency, equivalent to 93.9 % capacitance retention.

#### 5. Acknowledgement

The authors acknowledged the Technical Support of Advanced Chemistry Laboratory, Sheda Science and Technology Complex (SHESTCO) Abuja, Nigeria and Solid State Physics & Material Science Laboratory, University of Nigeria Nsukka.

#### References

- [1] Vinod, K.G., Ali, F., Shilpi, A., &Mahsa, N. (2018). Palladium oxiden nanoparticles supported on reduced graphene oxide and gold doped: Preparation, characterization and electrochemical study of supercapacitor electrode. *Journal of Molecular Liquids* 249, 61–65.
- [2] Bidhan, P., Sanjay R. D., Bhanu P. S., Babasaheb R. S. (2017). Free-standing flexible MWCNTs bucky paper: Extremely stable and energy efficient supercapacitive electrode. *Electrochimica Acta*, 249, 395–403.
- [3] Qian, J., Xiong, Y., Cao, Y., Ai X., & Yang, H. (2014). Influence of Particle Size Distribution on the Performance of Ionic Liquid-based Electrochemical Double Layer Capacitors *Nano Letters* 14, 1865–1869
- [4] Liu, Y., Zhang, N., Jiao, L., Tao Z., & Chen, J. (2015). Graphene-based supercapacitor with an ultrahigh energy density *Advance Functional Matter* 25, 214–220
- [5] Hsu, P.C., Chen, W.C., Tsai, Y.T. (2013). Fabrication of p-type SnO thin-film transistors by sputtering with practical metal electrodes. *Japanese Journal of Applied Physics* 52, 5,232-23.
- [6] Meher, SK., &Rao, G.R. (2011). Self-supported hydrothermal synthesis hollow  $\text{Co}_3\text{O}_4$  nanowire arrays with high supercapacitor capacitance. *Journal of Physical Chemistry C* 115, 156.
- [7] Alaa, A.A., &Hassanien A.S. (2015). Microstructure and crystal imperfections of nanosized  $\text{CdS}_x\text{Se}_{1-x}$  Thermally evaporated thin films. *Elsevier*, 85, 67-81,
- [8] Ali, S.M., Muhammad, J., Hussain, S.T., Bakar, S.A., Ashraf, M., &Naeem, U.R. (2013). Study of microstructural, optical and electrical properties of Mg doped SnO thin films. *Journal of Materials Science: Materials in Electronics*, 24, 2432–2437.
- [9] Augustyn, V., Come, J., Lowe, M.A., Kim, J.W., Taberna, P.L., Tolbert, S.H., Abruna, H.D., Simon, P., & Dunn, B. (2013). Pseudocapacitor oxide materials for high-rate electrochemical energy storage. *Nature Materials* 12, 518.
- [10] Beguin, F., Presser, V., Balducci, A., &Frackowiak, E. Carbon and electrolytes For advance Supercapacitor. (2014). *Advance matter* 2219, 26-28.
- [11] Bello, A., Barzegar, F., Momodu, D., Dangbegnon, J., Taghizadeh, F., &Manyala, N. (2015). Symetric supercapacitor based on porous 3D interconnected Carbon framework. *ElectrochimActa*, 386, 151.
- [12] Conway, B. (1999). *Electrochemical Supercapacitors: Scientific Fundamentals and Technological Applications*, Kluwer Academic Publishers, Plenum Press: New York, New York
- [13] Gao, Z., Wang, J., Li, Z., Yang, W., & Wang, B. (2011). Graphene nanosheet/NiAl layered double hydroxide composite as a novel electrode for a supercapacitor. *Chemical mater* 32, 3509.
- [14] Hoai, P. P., Thanh, G. L., Quang, T. T., Hoang H. N., Huynh, T. H., Hoang, T. T., & Tran V. C. (2017). Characterization of Ag-Doped P-Type SnO Thin Films Prepared by DC Magnetron Sputtering. *Journal of Nanomaterials*, 234-337.

[15] Junfu, L., James, O., Xianghui, H., & George Z. C. (2017). Faradaic processes beyond Nernst's law: functional theory assisted modelling of partial electron delocalisation and pseudocapacitance in graphene. *Chemistry Communication* 53, 10414.

[16] Largeot, C., Portet, C., Chmiola, J., Taberna, P.L., Gogotsi, Y., & Simon, P. (2008). Confinement, desolvation and electrosorption effects on the diffusion of ions in nanoporous carbon electrode. *Journal of American Chemical Society* 130, 2730.

[17] Lowsk, A.K., Cki, J.C., & Beker, B. (2008). Influence of grain size on deformation mechanism: an extension to nanocrystalline materials. *Dalton Transactions* 47, 6825.

[18] Madhu, C., Bose, V.C., Maniammal, A.S., Aiswarya, A.S., Biju, V. Effect of aging on nanostructure nickel samples. *BijuPhysica*, 421, 87.

[19] Martinelli, A., Palenzona, A., Putti, M., Ferdeghini, C. (2009). Microstructural transition in 1111 Prictides. *J.W.Lynn, Pengcheng Dai Physica C* 469.

[20] Nakazawa, K., Itoh, S., Matsunaga, T., Matsukawa Y., Satoh, Y., & Abe, H. (2014). Effect of dislocation and grain boundary on deformation mechanism in ultrafine-grain interstitial-free steel. *Material Science and Engineering* 61, 012125.

[21] Ozolin, V., Zhou F., & Asta, M. (2013). *Account of Chemical Research* 46, 1084-1093.

[22] Pandolfo, A.G., & Hollenkamp, A.F. (2006). Carbon properties and their role in supercapacitors. *Journal of Power Sources* 11, 157-160.

[23] Raymundo-Pinero, E., Kierzek, J., Lota, G., Gryglewicz, G., & Machnikowski, J. (2004). Electrochemical capacitor based on highly porous carbons prepared by KOH activator. *ElectrochimActa* 515, 49-52.

[24] Siamak, P.J., Alagarsamy, P., Boon, T.G., Hong, N.L. & Nay, M.H. (2015). Influence of particle size on performance of Nickel nanoparticles-based supercapacitor. *RSCAdvances* 5, 14010-14019.

DEVELOP

Depa

1. INTRO

The study result of as a com object ar people a vision ar To ensu tasks, te "lux". The lux meter(h A simp as per Measur solutio and ex

Corre